J. Microbiol. Biotechnol. (2008), **18**(9), 1572–1577

JOURNAL OF MICROBIOLOGY AND BIOTECHNOLOGY

Microbial Production and Characterization of Superparamagnetic Magnetite Nanoparticles by *Shewanella* sp. HN-41

Lee, Ji-Hoon[1†], Yul Roh[2], and Hor-Gil Hur[1]*

[1]*Department of Environmental Science and Engineering, and International Environmental Research Center, Gwangju Institute of Science and Technology, Gwangju 500-712, Korea*
[2]*Faculty of Earth Systems and Environmental Sciences, Chonnam National University, Gwangju 500-757, Korea*

Received: January 15, 2008 / Accepted: April 5, 2008

A facultative dissimilatory metal-reducing bacterium, *Shewanella* sp. strain HN-41, was used to produce magnetite nanoparticles from a precursor, poorly crystalline iron-oxyhydroxide akaganeite (β-FeOOH), by reducing Fe(III). The diameter of the biogenic magnetite nanoparticles ranged from 26 nm to 38 nm, characterized by dynamic light scattering spectrophotometry. The magnetite nanoparticles consisted of mostly uniformly shaped spheres, which were identified by electron microscopy. The magnetometry revealed the superparamagnetic property of the magnetic nanoparticles. The atomic structure of the biogenic magnetite, which was determined by extended X-ray absorption fine structure spectroscopic analysis, showed similar atomic structural parameters, such as atomic distances and coordinations, to typical magnetite mineral.

Keywords: Biogenic magnetite, superparamagnetism, dissimilatory metal-reducing bacteria

Over the past two decades, appreciation for the role of microbes in the intracellular and extracellular biomineralization of nanometer-sized minerals has grown. Among the diverse biogenic nanomaterials, magnetite has been attracting interests for biogeochemistry [9], evidence for extraterrestrial life on meteorites [1, 10], *etc.* Magnetite nanoparticles have many technological potentials for application, such as in magnetic-controlling devices, memory devices in electronic appliances, magnetic separation, drug delivery, hyperthermia treatment, magnetic resonance imaging (MRI) contrast enhancement, *etc.* [7, 11, 21, 26].

Magnetotactic bacteria are known to synthesize magnetite by a direct mechanism of mineralization [2, 5, 8]. They produce intracellular magnetite (magnetosomes) of high purity and crystallinity, which shows consistent morphologies and narrow grain-size distribution that are within single domain size ranges [17, 27]. Meanwhile, dissimilatory metal-reducing bacteria (DMRB) can also form magnetite by indirect means on or outside their cell walls [14, 18]. The extracellular magnetite is irregular in morphology and wide in grain-size distribution and extends into the superparamagnetic size range [17, 27]. There have been many studies on the magnetism and morphology of both biogenic magnetites [17, 27, 30], and most of the studies focused on the magnetosome magnetite formed by magnetotactic bacteria owing to its high purity and crystallinity. Despite the irregular and heterogeneous morphology of the magnetite nanoparticles produced by DMRB, those show superparamagnetic behavior [3], which is of interest for diverse applications owing to the loss of their magnetism when the external magnetic field is removed.

Here, we present the physical and chemical properties of the magnetite nanoparticles produced by a dissimilatory metal-reducing bacterium, *Shewanella* sp. strain HN-41 [13], including quantitative grain-size distribution, morphological shape, magnetic characteristics, and atomic level structure by extended X-ray absorption fine structure (EXAFS) spectroscopic analysis.

Materials and Methods

Preparation of Magnetite Precursor

Poorly crystalline Fe(III)-oxyhydroxide akaganeite nanoparticles was synthesized as a precursor for the bacterial production of magnetite [13]. In brief, the poorly crystalline akaganeite colloidal suspension was prepared by neutralizing 0.4 M $FeCl_3 \cdot 6H_2O$ solution to pH 7 with 10 N NaOH [13, 25]. The suspension was stirred overnight at room temperature and washed with Milli-Q water (18 MΩ cm), purified by a Milli-Q plus water system (Millipore Corp., Bedford, MA, U.S.A.) three times, and adjusted to ~0.7 M solution with the Milli-Q water followed by N_2 (100%)-flushing and anaerobic capping.

*Corresponding author
Phone: 82-62-970-2437; Fax: 82-62-970-2434;
E-mail: hghur@gist.ac.kr

†Present address: Biological Sciences Division, Pacific Northwest National Laboratory, Richland, Washington 99352, U.S.A.

Bacterial Media and Cultivation Conditions

Anaerobic HEPES-buffered defined medium [13] was used for the bacterial culture, and adjusted to pH 7.5 by using 10 N NaOH. Standard anaerobic culturing techniques were used throughout the study [15]. To produce magnetite particles, a facultative anaerobic dissimilatory metal-reducing bacterium, *Shewanella* sp. HN-41 [13], was incubated in the anaerobically prepared medium supplemented with the synthetic poorly crystalline akaganeite (~70 mM) and lactate (10 mM) from the anaerobically prepared stock solutions. All incubations were performed in the dark at 30°C.

Mineralogical Analyses

For the mineralogical analyses, the settled mineral residues were sampled from the culture bottles, collected by centrifugation at 2,300 ×*g* for 10 min (5415D, Eppendorf, Hamburg, Germany), and washed with anaerobic deionized water three times. The collected minerals were dried under anaerobic condition in the glove box (N_2:H_2:CO_2=90:5:5) (Coy Laboratory, Ann Arbor, MI, U.S.A.).

For electron microscopy, the washed samples were mounted on mixed cellulose ester filter or silicon-wafer for scanning electron microscopy (SEM) (FE-SEM S-4700; Hitachi, Tokyo, Japan) or Cu-grid for transmission electron microscopy (TEM) (JEM 2100F HR-TEM; JEOL, Tokyo, Japan), and dried in the glove box.

Dynamic light scattering (DLS) (DLS-7000AL; Otsuka Electronics, Osaka, Japan) analysis was adopted to examine the size distribution of the magnetite particles. To disperse the magnetite particles and reduce agglomeration of the nanoparticles in liquid, the magnetite nanoparticles were prepared as a ferrofluid [4]. The magnetite was mixed with a surfactant, aqueous tetramethyl-ammonium hydroxide solution (25%), which surrounds the magnetite nanoparticles with hydroxide anions and tetramethyl-ammonium cations to create an electrostatic repulsion between the particles in the solution [4]. The mixed solution was stirred with a magnetic stirring bar inside a hood for 30 min to remove excess ammonia from the solution. After stirring, the solution was poured into a beaker slowly and carefully while removing the stirring bar by using a strong block-shaped Nd-Fe-B magnet. The prepared magnetite ferrofluid solution was used for the analysis of DLS.

SQUID Magnetometry

The magnetic properties of the magnetite were investigated using a SQUID magnetometer (MPMS5; Quantum Design, San Diego, CA, U.S.A.) at a temperature ranging from 5 to 330 K under different applied magnetic fields. Two methods for the temperature-dependent magnetization of the nanoparticles were used. For the zero-field-cooled (ZFC) magnetization measurement (M_{ZFC}), the sample was first cooled down to 5 K without an applied magnetic field and then magnetization of the sample was measured from 5 to 330 K with the applied magnetic field. In the second case, for the field-cooled (FC) magnetization measurement (M_{FC}), the sample was cooled down to 6 K with the applied magnetic field and measurements of magnetic moment at each intermediate temperature were carried out.

Extended X-Ray Absorption Fine Structure (EXAFS) Spectroscopy

EXAFS spectra were collected *via* a laboratory-scale EXAFS spectroscopy system (R-XAS; Rigaku, Tokyo, Japan), which features an X-ray generator instead of a beamline source from traditional synchrotron radiation, and an absence of higher harmonics in the EXAFS spectra owing to the relatively low energy. The EXAFS spectra were all measured at room temperature in the conventional transmission mode. Spectra were collected from the Fe *K*-edge of the biogenic magnetite nanoparticles, and recorded from 6,670 to 8,220 eV with 1.0 to 5.0 eV steps according to the specified ranges. X-rays were generated at 14 kV and 20 mA with an LaB_6 filament and Mo as the target material. Data processing and analysis for the EXAFS spectra were performed by using the IFEFFIT package (version 1.2.6) [19]. The raw EXAFS spectra of the Fe *K*-edge of the biogenic magnetite nanoparticles were normalized to the edge-jump, after subtracting the backgrounds of the pre-edge regions estimated by the AUTOBK [20] algorithm in IFEFFIT. Fourier transforms of the EXAFS function [χ(k)] from wavenumber (k) to distance space (R) were performed with a weighting factor (k^2) and a Kaiser-Bessel window function to avoid ringing, in ranges of k from 2.0 to 9.58 Å^{-1}. The EXAFS data in large wavenumber regions were excluded to extract only the oscillatory parts. The experimental data were fitted in the *R*-space by the difference file technique, which was applied to resolve the different contributions of scattering atom pairs in the EXAFS data. The radial structure function (RSF) was suggested with no consideration of the phase shift. The local structure model around the Fe atom in the magnetite were expected from the atomic coordination distribution by the result of ATOMS [22] based on the reference magnetite [29], and the crystallographic data for the FEFF6 [23, 24] calculation was suggested (Table 1). In this EXAFS analysis, coordination numbers were fixed but bond lengths were optimized, and the three peaks of Fourier transformed data were fitted individually.

Table 1. Crystallographic data of standard magnetite for FEFF calculations.

Standard	Space group	Lattice parameter (Å)	Coordination number, N	Interatomic distance, R (Å)
Magnetite	Fd3m	a, b, c=8.3958	4 (O)	1.886
			12 (Fe)	3.481
			12 (O)	3.493

RESULTS AND DISCUSSION

Formation of Magnetite from Akaganeite

Shewanella sp. HN-41 (Fig. 1A) produced magnetite particles outside their cells from the poorly crystalline akaganeite by reducing Fe(III) to Fe(II) when the strain was incubated with lactate as an electron donor and carbon source under anaerobic condition, as suggested by Lee *et al.* [13]. The mineralogical identification by X-ray powder diffraction of the synthetic akaganeite and the biogenic magnetite was also suggested in the previous report [13].

Characterization of the Magnetite Nanoparticles

Lactate-grown strain HN-41 produced copious amount of Fe_3O_4 nanoparticles (Fig. 1). SEM images of the magnetite showed nano-sized spherical forms (Figs. 1B and 1C). TEM observation showed crystalline magnetite nanoparticles

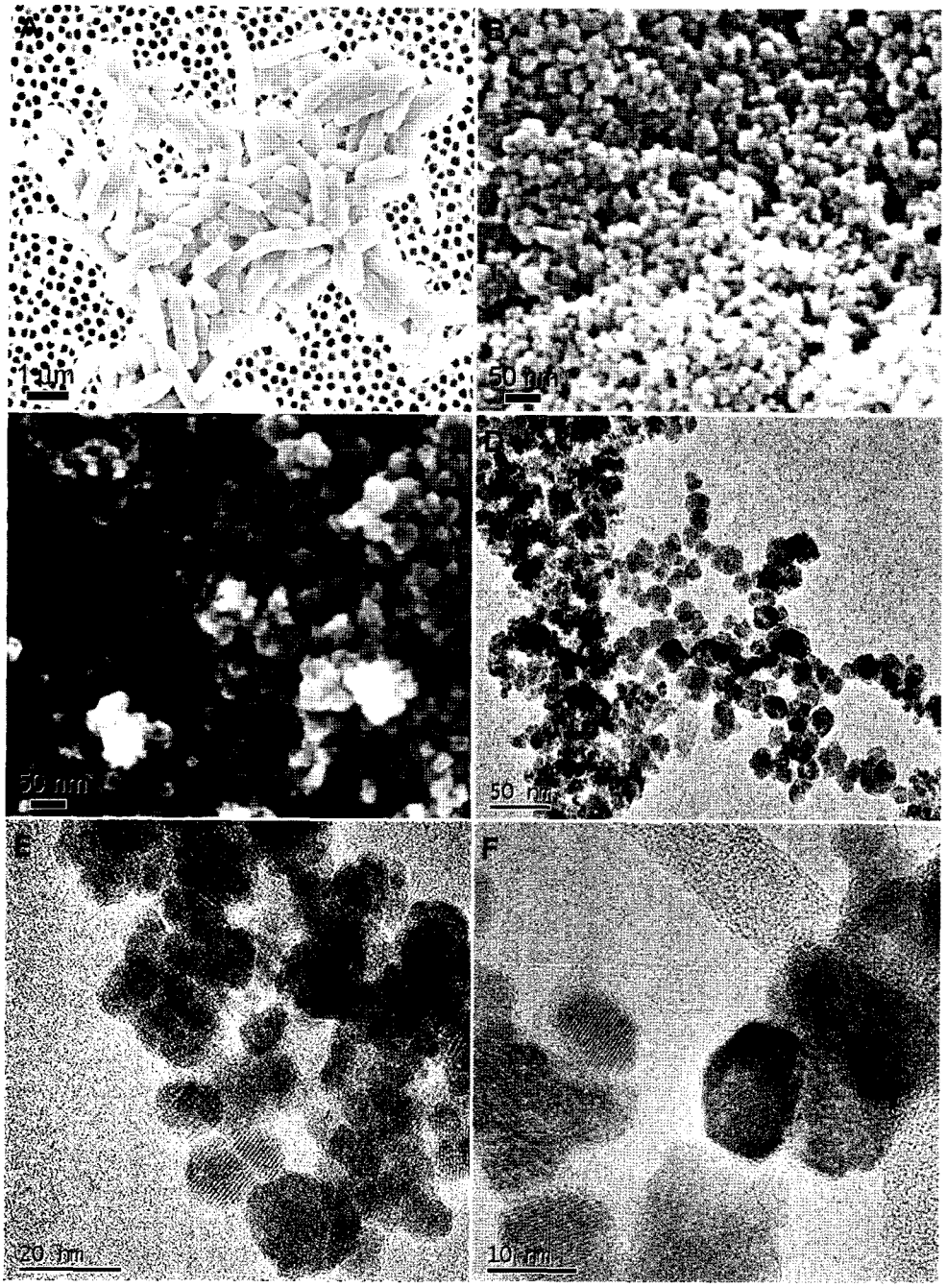

Fig. 1. Electron microscopic images of the strain HN-41 and magnetite nanoparticles.
A: *Shewanella* sp. HN-41; **B** and **C**: SEM images of magnetite nanoparticles; **D**, **E**, and **F**: TEM images of magnetite nanoparticles.

(Figs. 1D, 1E, and 1F) and a hexagonal structure as well (Fig. 1F), which is an authentic image for magnetite. A dynamic light scattering (DLS) spectrophotometer was used to investigate the size distribution of the magnetite nanoparticles prepared as a ferrofluid [4]. The diameter distribution of the magnetite nanoparticles was 26.7–37.7 nm with an average of 28.8±3.4 nm (Fig. 2). The relative standard deviation of the diameter distributions of the magnetite nanoparticles ranged from 11.4% to 20.2% from triplicate measurements.

Moskowitz *et al.* [17] and Sparks *et al.* [27] compared magnetites produced by magnetotactic bacteria and DMRB, and suggested that the magnetotactic bacterium strain MV-1 produced well-defined crystalline magnetite with narrow grain-size distributions [length: 21–74 nm (53±10.86 nm); width: 12–54 nm (35±7.86 nm)] [27], whereas *Geobacter metallireducens* GS-15 produced irregular magnetite with wide grain-size distributions [carbonate-buffer particles, length: 8.11–22.47 nm (14±3.02 nm), width: 5.81–15.72 nm (11±2.51 nm); phosphate-buffer particles, length: 6.25–

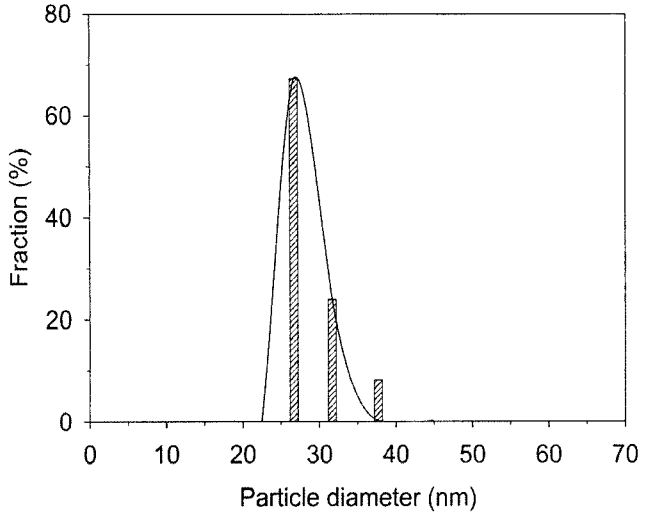

Fig. 2. Size distribution measured by DLS spectroscopy of the biogenic magnetite.
The solid line represents the best fit to the distribution using a log-normal function.

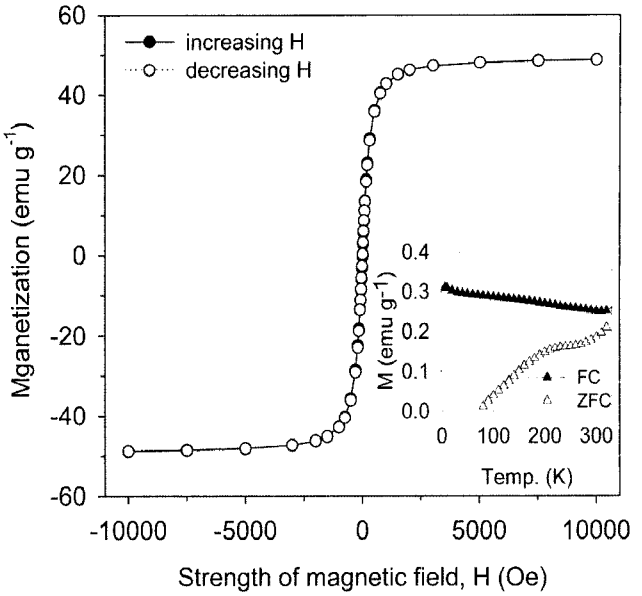

Fig. 3. Magnetization of the magnetite nanoparticles by SQUID magnetometry.
Magnetization loop M(H) at 310 K, anhysteric behavior of superparamagnetic materials (Inset: temperature dependence of magnetization at an applied field of 10 Oe). The blocking temperature is over or around 330 K.

23.00 nm (12±3.40 nm), width: 5.33–20.16 nm (10±2.90 nm)] [27]. As compared with the previous results, *Shewanella* sp. HN-41 produced a relatively regular sphere shape with less wide size distribution.

Fig. 3 shows the magnetization curve of the magnetite nanoparticles over the outer magnetic fields at 310 K measured by the SQUID magnetometer. The *M-H* curve is completely reversible, which is anhysteric but still sigmoidal, indicating a typical superparamagnetic behavior [16] for the magnetite nanoparticles, as evidenced by zero coercivity and remanence on the magnetization loop. A saturation magnetization of 48.77 emu/g was determined for the magnetite nanoparticles. The splitting of the zero-field-cooled (ZFC) and field-cooled (FC) curves is very pronounced, providing easy and unique determination of the blocking temperature T_B, over which either the amount of the magnetic order falls until it eventually loses all magnetization, or a magnetic nanostructure loses its preferred magnetization direction. The inset in Fig. 3 shows the temperature dependence of M_{ZFC} and M_{FC} for the magnetite nanoparticles at the applied field of H=10 Oe. Whereas M_{FC} did not change much in the whole temperature range (5 to 330 K), M_{ZFC} decreased with decreasing temperature, suggesting that T_B is approximately 200 to 210 K, above which the magnetization direction of a nanostructure will fluctuate randomly in the absence of any external magnetic field.

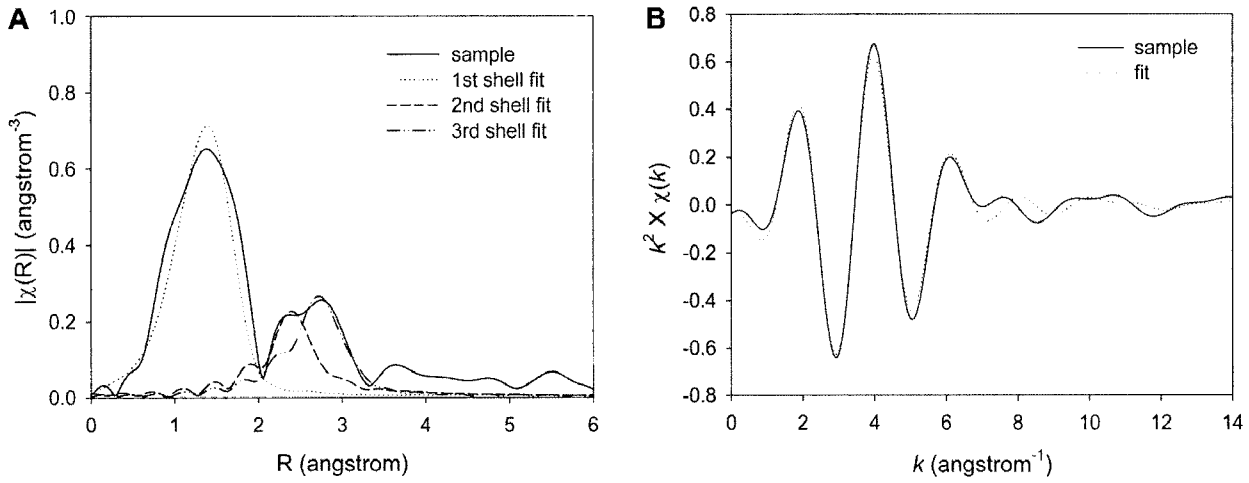

Fig. 4. Fourier-filtered EXAFS data for the biogenic magnetite.
A. Magnitude of the Fourier transform (FT) of EXAFS data and the best-fit models (R, radial distance: uncorrected for electron phase shift). **B.** k^2-weighted $\chi(k)$ (EXAFS) functions for the 1st shells. Solid lines represent the experimental data, and dotted lines are the fits.

Table 2. EXAFS analysis results of the biogenic magnetite.

Sample	Shell	Atomic pair	Scattering type	R (Å)	N	σ^2 (Å)[a]	ΔE_0 (eV)[b]	r factor[c]
Biogenic magnetite	1st	Fe-O	SS	2.016	4	0.0188	-4.72	0.0911
	2nd	Fe-O-O-Fe	DS[e] (triangle)	3.092	12	0.0150	-9.51	0.0091
	3rd	Fe-O	SS	3.336	12	0.0029	-3.97	0.0251

[a]Debye-Waller factor, mean square variation of R, indicating the variance in the absorber-scatterer distance.
[b]Edge-jump.
[c]Indicating quality of the fit.
[d]Single scattering.
[e]Double scattering.

Atomic Structure of Magnetite by EXAFS

EXAFS spectroscopy was employed to identify the coordination environment around the Fe atom of the magnetite [23]. The RSF and k^2-weighted fourier-filtered EXAFS function $\chi(k)$ of Fe *K*-edge spectra were drawn against interatomic distance (*R*) and wavenumber (k), respectively, in Fig. 4. The first peak-fitting for the biogenic magnetite nanoparticles explains the same 4 Fe-O single-scattering paths, which indicates the tetrahedral structure around the center Fe atom (Fig. 4A, Table 2). The second peak in the magnetite FT data was fitted by 12 different directional triangle Fe-O-O-Fe double-scattering paths in the tetrahedron, and the third peak represented 12 Fe-O single-scattering paths resulting from the nearest 12 oxygen atoms around the central Fe (Fig. 4A, Table 2). These results suggest that the local structure around Fe agrees with a reference mineral magnetite [29]. All of the optimized structural parameters in the neighborhood of the absorber Fe atom for the biogenic magnetite are summarized in Table 2. The mean square variation of interatomic distance (R), Debye-Waller factor (σ^2), was of reasonable value, and a parameter indicating the quality of the fit, r factor, was less than 0.0911.

We have provided characterization of substantially sphere-type superparamagnetic magnetite (Fe_3O_4) nanoparticles produced by a dissimilatory metal-reducing bacterium, *Shewanella* sp. HN-41, under the anaerobic condition. Owing to the versatility of genus *Shewanella*, one of the DMRB, as suggested by Tiedje [28], it has been studied in many fields of applications such as microbial fuel cells [6, 12]. In an attempt to synthesize Fe_3O_4 and MFe_2O_4 nanoparticles with low energy input as well, the production method by using DMRB is likely to be an alternative choice.

Acknowledgments

We thank Dr. Hong-Ryun Jung (Chonnam National University) for her kind help and advice on EXAFS data acquisition and analysis, and Dr. Robert A. Kanaly for his critical editing and advice. This work was supported in part by the 21C Frontier Microbial Genomics and Applications Center Program of the Ministry of Science and Technology, and the National Core Research Center program (Grant no. R15-2003-012-02002-0) of the Ministry of Science and Technology, Korea.

References

1. Barber, D. J. and E. R. D. Scott. 2002. Origin of supposedly biogenic magnetite in the Martian meteorite Allan Hills 84001. *Proc. Natl. Acad. Sci. USA* **99:** 6556–6561.
2. Bazylinski, D. A., R. B. Frankel, and H. W. Jannasch. 1988. Anaerobic production of magnetite by a marine magnetotactic bacterium. *Nature* **334:** 518–519.
3. Bazylinski, D. A. and B. M. Moskowitz. 1997. Microbial biomineralization of magnetic iron minerals: Microbiology, magnetism and environmental significance, pp. 181–223. *In* J. F. Banfield and K. H. Nealson (eds.), *Geomicrobiology: Interactions Between Microbes and Minerals*. The Mineralogical Society of America, Washington, D.C.
4. Berger, P., N. B. Adelman, K. J. Beckman, D. J. Campbell, A. B. Ellis, and G. C. Lisensky. 1999. Preparation and properties of an aqueous ferrofluid. *J. Chem. Educ.* **76:** 943–948.
5. Blackemore, R. P. 1975. Magnetotactic bacteria. *Science* **190:** 377–379.
6. Chang, I. S., H. Moon, O. Bretschger, J. K. Jang, H. I. Park, K. H. Nealson, and B. H. Kim. 2006. Electrochemically active bacteria (EAB) and mediatorless microbial fuel cells. *J. Microbiol. Biotechnol.* **16:** 163–177.
7. Choi, J.-W., B.-K. Oh, Y.-K. Kim, and J. Min. 2007. Nanotechnology in biodevices. *J. Microbiol. Biotechnol.* **17:** 5–14.
8. Frankel, R. B., R. P. Blackemore, and R. S. Wolfe. 1979. Magnetite in freshwater magnetotactic bacteria. *Science* **203:** 1355–1356.
9. Fredrickson, J. K., J. M. Zachara, D. W. Kennedy, H. Dong, T. C. Onstott, N. W. Hinman, and S.-M. Li. 1998. Biogenic iron mineralization accompanying the dissimilatory reduction of hydrous ferric oxide by a groundwater bacterium. *Geochim. Cosmochim. Acta* **62:** 3239–3257.
10. Friedmann, E. I., J. Wierzchos, C. Ascaso, and M. Winklhofer. 2001. Chains of magnetite crystals in the meteorite ALH84001: Evidence of biological origin. *Proc. Natl. Acad. Sci. USA* **98:** 2176–2181.
11. Hutten, A., D. Sudfeld, I. Ennen, G. Reiss, W. Hachmann, U. Heinzmann, *et al.* 2004. New magnetic nanoparticles for biotechnology. *J. Biotechnol.* **112:** 47–63.

12. Kim, B.-H., H.-J. Kim, M.-S. Hyun, and D.-H. Park. 1999. Direct electrode reaction of Fe(III)-reducing bacterium, *Shewanella putrefaciens*. *J. Microbiol. Biotechnol.* **9:** 127–131.
13. Lee, J.-H., Y. Roh, K.-W. Kim, and H.-G. Hur. 2007. Organic acid-dependent iron mineral formation by a newly isolated iron-reducing bacterium, *Shewanella* sp. HN-41. *Geomicrobiol. J.* **24:** 31–41.
14. Lovley, D. R., J. F. Stolz, G. L. Nord, and E. J. P. Phillips. 1987. Anaerobic production of magnetite by a dissimilatory iron-reducing microorganism. *Nature* **330:** 252–254.
15. Miller, T. L. and M. J. Wolin. 1974. A serum bottle modification of the Hungate technique for cultivating obligate anaerobes. *Appl. Microbiol.* **27:** 985–987.
16. Morrish, A. H. 2001. *The Physical Principles of Magnetism*. IEEE Press, New York.
17. Moskowitz, B. M., R. B. Frankel, D. A. Bazylinski, H. W. Jannasch, and D. R. Lovley. 1989. A comparison of magnetite particles produced anaerobically by magnetotactic and dissimilatory iron-reducing bacteria. *Geophys. Res. Lett.* **16:** 665–668.
18. Myers, C. R. and K. H. Nealson. 1990. Iron mineralization by bacteria: Metabolic coupling of iron reduction to cell metabolism in *Alteromonas putrefaciens* MR-1, pp. 131–149. *In* R. B. Frankel and R. P. Blakemore (eds.), *Iron Biominerals*. Plenum Press, New York.
19. Newville, M. 2001. IFEFFIT: Interactive XAFS analysis and FEFF fitting. *J. Synchrotron Rad.* **8:** 322–324.
20. Newville, M., P. Livins, Y. Yacoby, E. A. Stern, and J. J. Rehr. 1993. Near-edge X-ray-absorption fine structure of Pb: A comparison of theory and experiment. *Phys. Rev. B* **47:** 14126–14131.
21. Pankhurst, Q. A., J. Connolly, S. K. Jones, and J. Dobson. 2003. Applications of magnetic nanoparticles in biomedicine. *J. Phys. D Appl. Phys.* **36:** R167–R181.
22. Ravel, B. 2001. ATOMS: Crystallography for the X-ray absorption spectroscopist. *J. Synchrotron Rad.* **8:** 314–316.
23. Rehr, J. J. and R. C. Albers. 2000. Theoretical approaches to X-ray absorption fine structure. *Rev. Mod. Phys.* **72:** 621–654.
24. Rehr, J. J., J. M. D. Leon, S. I. Zabinsky, and R. C. Albers. 1991. Theoretical X-ray absorption fine structure standards. *J. Am. Chem. Soc.* **113:** 5135–5140.
25. Schwertmann, U. and R. M. Cornell. 2000. *Iron Oxides in the Laboratory: Preparation and Characterization*, 2nd Ed. Wiley-VCH, Weinheim.
26. Shinkai, M. 2002. Functional magnetic particles for medical application. *J. Biosci. Bioeng.* **94:** 606–613.
27. Sparks, N. H. C., S. Mann, D. A. Bazylinski, D. R. Lovley, H. W. Jannasch, and R. B. Frankel. 1990. Structure and morphology of magnetite anaerobically-produced by a marine magnetotactic bacterium and a dissimilatory iron-reducing bacterium. *Earth Planet. Sci. Lett.* **98:** 14–22.
28. Tiedje, J. M. 2002. *Shewanella* - the environmentally versatile genome. *Nat. Biotechnol.* **20:** 1093–1094.
29. Wechsler, B. A., D. H. Lindsley, and C. T. Prewitt. 1984. Crystal structure and cation distribution in titanomagnetites ($Fe_{3-x}Ti_xO_4$). *Am. Mineral.* **69:** 754–770.
30. Weissa, B. P., S. S. Kim, J. L. Kirschvink, R. E. Kopp, M. Sankaran, A. Kobayashi, and A. Komeili. 2004. Ferromagnetic resonance and low-temperature magnetic tests for biogenic magnetite. *Earth Planet. Sci. Lett.* **224:** 73–89.